Available online at www.sciencedirect.com
ScienceDirect
Pattern Recognition 41 (2008) 1785–1798
PATTERN RECOGNITION
THE JOURNAL OF THE PATTERN RECOGNITION SOCIETY
www.elsevier.com/locate/pr

Boundary based shape orientation

Joviša Žunić[a,*,1], Miloš Stojmenović[b]

[a]*Computer Science Department, Exeter University, Harrison Building, Exeter EX4 4QF, UK*
[b]*SITE, University of Ottawa, Ottawa, Ontario, Canada K1N 6N5*

Received 2 May 2007; received in revised form 4 October 2007; accepted 8 October 2007

Abstract

The computation of a shape's orientation is a common task in the area of computer vision and image processing, being used for example to define a local frame of reference and is helpful for recognition and registration, robot manipulation, etc. It is usually an initial step or a part of data preprocessing in many image processing and computer vision tasks. Thus, it is important to have a good solution for shape orientation because an unsuitable solution could lead to a big cumulative error at the end of the computing process. There are several approaches to the problem—most of them could be understood as the 'area based' ones, or at least they do not take into account all the boundary points (if a shape orientation measure is based on its encasing rectangle, only the convex hull points count, for example). Thus, the demand for a pure 'boundary based' method, where the orientation of the shape is dependent on the boundary points seems to be very reasonable. Such a method is presented in this paper. We are initially focused on the shapes having polygonal boundaries. We define the orientation of a polygonal shape by the line that maximises the total sum of squared lengths of all the boundary edge projections onto this line. The advantages and limitations of the new method are analysed.

Next, we suggested how the method can be adapted in order to be applicable to a wider class than the initial method is. Finally, we introduced another modification of the method in such a way that the modified method can be applied to shapes with arbitrary boundaries. Several illustrative experiments are provided.

Keywords: Shape; Orientation; Image processing; Computer vision

1. Introduction

Many image processing and shape analysis tasks start with a normalisation procedure [1–3]. For a successful application (in robotics, medical imaging, industry inspection tasks, etc.) it is important that the position and orientation of the shape under consideration are properly determined. Shape position and orientation define the frame of reference. Usually, the shape position is defined by its center of gravity, which is a very common approach. On the other hand, computing the orientation is not a straightforward task and consequently, there are several approaches in defining the shape orientation.

In fact, due to the variety of shapes as well as the diversity of applications there is probably no single method for computing shape orientation that could be efficiently and successfully applicable to all shapes. For that reason, several methods have been developed [4–10]. Different techniques have been used, including those based on geometric moments, complex moments, and principal component analysis, for example. The suitability of those methods strongly depends on the particular situation to which they are applied, as they each have their relative strengths and weaknesses.

Particular problems arise when working with symmetric shapes that obviously do not have a uniquely defined orientation. It is reasonable to assume that for each M-fold symmetric shape there are M concurrent directions that define the shape orientation. Note that rotation-symmetric and reflective-symmetric shapes appear very often not only in industry (as machine made products) but also in nature (e.g. human faces, crystals). The related problems (a detected symmetry axis

* Corresponding author. Tel.: +44 1392 26 4044; fax: +44 1392 26 4067.
E-mail addresses: J.Zunic@ex.ac.uk (J. Žunić), mstoj075@site.uottawa.ca (M. Stojmenović).
[1] Also with the Mathematical Institute, Serbian Academy of Sciences and Arts, Belgrade.

0031-3203/$30.00 © 2007 Elsevier Ltd. All rights reserved.
doi:10.1016/j.patcog.2007.10.007

could define shape orientation, for example) are intensively studied [6,7,9–15], as well.

It is worth mentioning the practical value of orientability in human visual perception. For instance, orientable shapes can be matched more quickly than shapes with no distinct axis [16].

The majority of the existing methods for computing the orientation are 'area based'—i.e. the computation takes into account all points that belong to the shape not only the boundary points. Among those area based methods, the most standard one says that shape orientation is determined by its axis of the least second moment of inertia [1–3]. The axis of the least second moment of a shape is defined as a line that minimises the integral of the squared distances of the shape points to the line. When working with shapes represented by a set of discrete points (set of pixels, for example) then the 'integral' should be replaced with the 'sum'. Obviously, the method is motivated very naturally. Also, because it is area based, the standard method is very robust with respect to noise and boundary defects. Moreover, it is simple to compute in both 'real' and 'discrete' versions—even the closed formulas for the computation of the orientation could be derived in both versions. For example, if $\mathcal{O}_{st}(S)$ denotes the orientation of the shape S computed by the standard method (i.e., $\mathcal{O}_{st}(S)$ is the slope of the axis of the last second moment of S) then

$$\frac{\sin(2\cdot\mathcal{O}_{st}(S))}{\cos(2\cdot\mathcal{O}_{st}(S))} = \frac{2\cdot\iint_S\left(x-\frac{\iint_S x\,\mathrm{d}x\,\mathrm{d}y}{\iint_S \mathrm{d}x\,\mathrm{d}y}\right)\cdot\left(y-\frac{\iint_S y\,\mathrm{d}x\,\mathrm{d}y}{\iint_S \mathrm{d}x\,\mathrm{d}y}\right)\mathrm{d}x\,\mathrm{d}y}{\iint_S\left(x-\frac{\iint_S x\,\mathrm{d}x\,\mathrm{d}y}{\iint_S \mathrm{d}x\,\mathrm{d}y}\right)^2\mathrm{d}x\,\mathrm{d}y-\iint_S\left(y-\frac{\iint_S y\,\mathrm{d}x\,\mathrm{d}y}{\iint_S \mathrm{d}x\,\mathrm{d}y}\right)^2\mathrm{d}x\,\mathrm{d}y}. \quad (1)$$

The problem is that there are many situations when this method does not give any answer as to what the shape orientation should be. There are many regular and irregular shapes where this standard method does not work [10,17]. M-fold ($M>2$) rotationally symmetric shapes are well known as shapes that cannot be oriented by the standard method. A use of higher order moments of inertia to determine the orientation of such shapes is proposed in Ref. [10]. Some useful properties of the method proposed in Ref. [10] are proven in Ref. [17]. The same paper gives a particular attention to the situations where the odd-order moments are used. Thus, sometime shape orientation tasks do not perform well because they do not fit well with a particular application in which they are used, but sometimes they could not perform well simply because of the nature of the considered shape. Regarding this problem, a new shape descriptor, named as *shape orientability*, is introduced in Ref. [18]. Such a new shape descriptor should indicate is the computed shape orientation an inherent property of the considered shape or the computed shape orientation results from digitisation and noise effects, for example. The new orientability measure is tested on both real and synthetic examples and it performs well. Particularly, it is invariant with respect to similarity transformations and the lowest possible orientability is assigned to a circle, while the highest possible orientability is assigned to a straight line segment.

Also, while in many situations the robustness of a method is a desirable property sometimes it could be a disadvantage. It could happen that some (by the standard method) "nonorientable" shapes could be oriented by existing narrow intrusions into the shape interior or by scribble details on them. Those details correspond to a relatively small percentage of pixels (when working with digital images) and their impact is not easily detectable by robust methods. In this paper we present a method where the orientation is computed based on the shape boundary and consequently could overcome such problems. In a typical situation, the complete boundary is taken into account—not only parts belonging to the convex hull of the considered shape [19,20], for example. The method can be applied to imperfect data—i.e. to shapes whose boundaries are partially detected or to shapes where small details are considered as boundary parts.

The paper is organized as follows. The new method for computing the orientation of polygonal shapes is described in Section 2. The method is analysed in detail in Section 3. Sections 4 and 5 give some modifications of the method. These modifications are presented in order to satisfy the additional demands that shape orientation methods should have depending on the situations that they are applied to. Section 6 contains concluding remarks.

2. Boundary based polygonal shape orientation

In this section we define a new method for polygonal shapes orientation. We do not restrict ourselves to polygonal shapes. In real image processing tasks we deal with digital data where the objects are presented by sets of sample points (e.g. pixels) and consequently, there is always an inherent loss of information about the boundaries of the original shapes. In most situations, the equations (or other precise descriptions) of shape boundaries remain unknown. In order to preserve easier data manipulation, shape boundaries are usually piecewise approximated with straight line segments, conic arcs, or spline arcs. Of course, approximating the boundary by a number of straight line segments (i.e. a use of polygonal approximation) is algorithmically simplest and computationally fastest.

Another argument for using polygonal approximations is that there are a variety of good algorithms for polygonal approximations of discrete shapes (for an overview see [21]).

Here we define the orientation $\mathcal{O}_{new}(P)$ of a polygonal shape P by the direction that maximises the total sum of the squared lengths of the projections of all the shape edges onto a line defined by this direction—see Fig. 1 for an illustration. The formal definition follows.

Definition 2.1. Let **P** be a shape with a polygonal boundary P. The orientation $\mathcal{O}_{new}(P)$ of **P** is defined by the angle α such that the total sum

$$F(\alpha, P) = \sum_{e \text{ is an edge of } P} |\mathbf{pr}_{\vec{a}}(e)|^2 \quad (2)$$

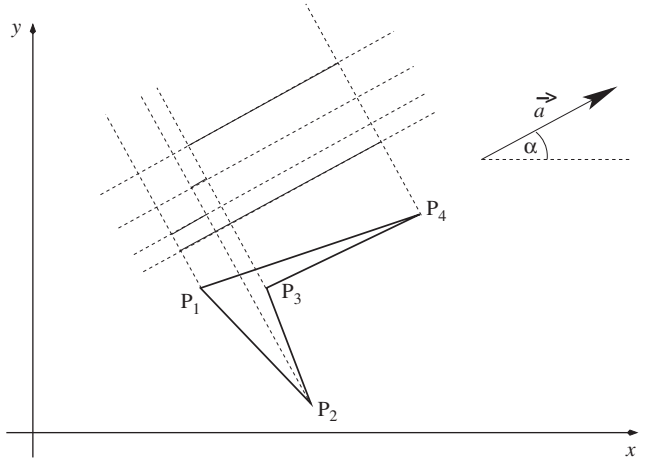

Fig. 1. Projections of the edges of the polygonal shape (having vertices P_1, P_2, P_3, P_4) onto lines having the slope α are presented.

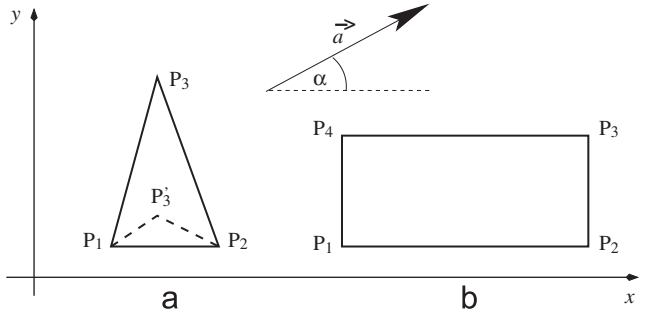

Fig. 2. The computed orientation $\mathcal{O}_{new}(\triangle P_1P_2P_3)$ is 90°. The computed orientation $\mathcal{O}_{new}(\triangle P_1P_2P_3')$ is 0°. The computed orientation $\mathcal{O}_{new}(P_1P_2P_3P_4)$ is 0°.

of squared lengths of projections of the edges of P onto a line having the slope α is maximal.

It is clear that new definition is naturally motivated. Also, in some canonical cases, when the orientation of polygonal shape seems to be straightforward, the method gives the expected results. The orientation of a rectangle is expected to be coincident with its longer edges, while the orientation of a symmetric triangle having a very long height should be coincident with its symmetry axis, for example. That is exactly what happens when the new method is applied. Without loss of generality we can assume that an edge of the considered rectangle and one edge of the considered triangle are parallel to the x-axis—for notations we refer to Fig. 2.

- For the rectangle $P_1P_2P_3P_4$ let $|P_1P_2| = |P_3P_4| = p$ and $|P_2P_3| = |P_4P_1| = q$. The sum of the squared projections of the edges onto a line having the slope α is

$$2 \cdot p^2 \cdot \cos^2\alpha + 2 \cdot q^2 \cdot \sin^2\alpha = 2 \cdot (p^2 - q^2) \cdot \cos^2\alpha + 2 \cdot q^2.$$

Consequently:
  - If $p > q$ the maximum is $2 \cdot p^2$ and it is reached for $\alpha = 0$, i.e., the rectangle is oriented in accordance with the longer edges.
  - If $p < q$ the maximum is $2 \cdot q^2$ and it is reached for $\alpha = \pi/2$ and, again, the rectangle is oriented in accordance with the longer edges.
  - If $p = q$ then the rectangle degenerates into a square and the method does not suggest what the orientation should be. The sum of the squared projection of edges is the same for all α. The orientation of rotationally symmetric shapes (as a square is) will be discussed in more details later on.
- For the triangle $\triangle P_1P_2P_3$ let $\beta = \angle(P_2P_1P_3) = \angle(P_1P_2P_3)$. The sum of the squared projections of the edges onto a line having the slope α is

$$q^2 \cdot \cos^2\alpha + p^2 \cdot \cos^2(\beta + \alpha) + p^2 \cdot \cos^2(\beta - \alpha),$$

where the p denotes the length of the edges P_3P_1 and P_2P_3 while q denotes the length of P_1P_2. Taking into account $\cos\beta = q/2p$ and by using elementary transformations the total sum of squares of the edge projections can be expressed as

$$2 \cdot (q^2 - p^2) \cdot \cos^2\alpha + 2 \cdot p^2 \cdot \left(1 - \frac{q^2}{4 \cdot p^2}\right).$$

So,
  - If $q < p$ then the maximum is reached for $\alpha = \pi/2$ and the orientation coincides with the axis of symmetry.
  - If $q > p$ then the maximum is reached for $\alpha = 0$ and the orientation is orthogonal to the axis of symmetry.
  Note: The obtained orientation is debatable if p is close to q, but it is very acceptable if q is much bigger than p. Particularly, in the limit case when $p \to q/2$ the triangle degenerates into a horizontal line segment whose measured orientation should be 0°, as given by the method.
  - If $q = p$ the sum of the squared edge projections is $2p^2 - q^2/2$ and it does not depend on α. Consequently the method does not tell what the orientation should be. Once again, M-fold rotationally symmetric shapes (such as a regular triangle) will be considered later on.
- It is worth mentioning that the exactly same orientations are obtained if the shape bounded by $\triangle P_1P_2P_3$ is oriented by the standard method.

In the previous two simple cases the orientation was easy to compute. The question is: *How does the method work in the case of an arbitrary polygonal area*? We will show that the method can be applied easily to all polygonal shapes. Furthermore, it is not solely applicable to closed polygonal lines, which can be of interest when working with incomplete data. i.e. when some boundary parts are missed or are not extracted properly. Also, there is a formal characterisation of the

situations when the method does not tell us what the orientation should be. This is a very desirable property. We proceed with the following theorem.

Theorem 2.1. *Let P be an n-gon with edges e_i, $i = 1, \ldots, n$. Also, let α_i (for $i = 1, \ldots, n$) denote the angle between e_i and the x-axis. If the total sum*

$$F(\alpha, P) = \sum_{i=1}^{n} |\mathbf{pr}_{\vec{a}}(e_i)|^2$$

of the squared lengths of the projections of the edges e_i onto a line having slope α reaches its maximum then

$$\tan(2 \cdot \alpha) = \frac{\sum_{i=1}^{n} |e_i|^2 \sin(2\alpha_i)}{\sum_{i=1}^{n} |e_i|^2 \cos(2\alpha_i)}. \tag{3}$$

Proof. Let $\vec{a} = (\cos\alpha, \sin\alpha)$ be the unit vector in the direction α, while e_i and α_i ($i = 1, \ldots, n$) are as stated in the theorem. The length of the projection $\mathbf{pr}_{\vec{a}}(e_i)$ of the edge e_i onto a line having slope α is

$$\begin{aligned} |\mathbf{pr}_{\vec{a}}(e_i)| &= |e_i| \cdot |(\cos\alpha_i \cos\alpha + \sin\alpha_i \sin\alpha)| \\ &= |e_i| \cdot |\cos(\alpha_i - \alpha)|, \end{aligned}$$

and the function that should be minimised (in order to compute the orientation of P) is

$$F(\alpha, P) = \sum_{i=1}^{n} |\mathbf{pr}_{\vec{a}}(e_i)|^2 = \sum_{i=1}^{n} |e_i|^2 \cos^2(\alpha_i - a). \tag{4}$$

The maximum of $F(\alpha, P)$ can be computed in a standard manner. The first derivative $\mathrm{d}F(\alpha, P)/\mathrm{d}\alpha$ can be expressed as

$$\begin{aligned} \frac{\mathrm{d}F(\alpha, P)}{\mathrm{d}\alpha} &= \sum_{i=1}^{n} |e_i|^2 \sin(2\alpha_i - 2\alpha) \\ &= \sum_{i=1}^{n} |e_i|^2 (\sin(2\alpha_i)\cos(2\alpha) - \cos(2\alpha_i)\sin(2\alpha)). \end{aligned} \tag{5}$$

Setting

$$\frac{\mathrm{d}F(\alpha, P)}{\mathrm{d}\alpha} = 0$$

we obtain that the angle α for which $F(\alpha, P)$ reaches the maximum satisfies the equality

$$\frac{\sin(2\alpha)}{\cos(2\alpha)} = \frac{\sum_{i=1}^{n} |e_i|^2 \sin(2\alpha_i)}{\sum_{i=1}^{n} |e_i|^2 \cos(2\alpha_i)},$$

which completes the proof. □

At the end of this section, it is worth giving three remarks that follow directly from the proof of the above given theorem.

Remark 1. Since $F(\alpha, P)$ is a continuous function, it reaches its extreme values on the closed interval $[0, 2\pi]$. For a given polygon P those extreme values are easy to compute in accordance with Eq. (3). If the maximum is reached at point $\alpha = \alpha_0$ then the minimum is reached at the point $\alpha = \alpha_0 + \pi/2$.

Remark 2. Due to the simplicity of the method it is expected that there are situations when the method does not give an answer regarding what the shape orientation should be. Incidentally, this was already shown in the case of a regular triangle and in the case of a square. Now we can give a formal characterisation of shapes for which the method does not work. Let P be a shape with a polygonal boundary. Looking at Eq. (5) we can see that $\mathrm{d}F(\alpha, P)/\mathrm{d}\alpha = 0$ (i.e. $F(\alpha, P) = \textit{constant}$) is equivalent to

$$\sum_{i=1}^{n} |e_i|^2 \cos(2\alpha_i) = 0 \quad \text{and} \quad \sum_{i=1}^{n} |e_i|^2 \sin(2\alpha_i) = 0. \tag{6}$$

That implies that Eq. (6) is the "necessary and sufficient condition" for $F(\alpha, P) = \textit{constant}$. Consequently, if Eq. (6) holds, the method does not suggest any particular direction as a candidate for the orientation of P. Later on we will show that $\mathrm{d}F(\alpha, P)/\mathrm{d}\alpha = 0$ holds for all shapes having more than two axes of symmetry or more generally, for all M-fold rotationally symmetric shapes, with $M > 2$.

Remark 3. Theorem 2.1 holds if P is an arbitrary polygonal curve (not necessarily a closed polygon). Moreover, the statement is valid if P consists of several not necessarily connected polygonal arcs. That is of importance when working with shapes whose orientation can be defined by scribble details.

3. Discussion and some examples

In this section we illustrate how the method works in practice. For each shape presented in Fig. 3 both, orientation $\mathcal{O}_{new}(P)$ computed by the new method and orientation $\mathcal{O}_{st}(P)$ computed by the standard method (the numbers in the brackets) are given. It is obvious that in the case of essential intrusions or in the case of long thin details a big difference between two computed orientations is possible. For instance, the impact of the trunk position change is much higher if the sketch of elephant is oriented by the new method than if it is oriented by the standard method (see shapes (a1) and (a2)). Also, the new method gives that the orientation $\mathcal{O}_{new}(P)$ of the sketch of rabbit strongly depends on the position of its ears—such an impact is lower if the standard method is applied (shapes (a3) and (a4)). The essential difference in the intrusion position of the shapes (a5) and (a6) cannot be detected by the standard method (for both shapes the computed orientation is 110°), while such a change has a big impact on the computed orientation if the new method is applied.

The first four examples in the second row illustrate a very useful property of the new method which does not hold if the standard method is applied. A man's silhouette (shape (b1)) has the same computed orientation 91° if both methods are applied. If the orientation of a compound shape (shape (b2))

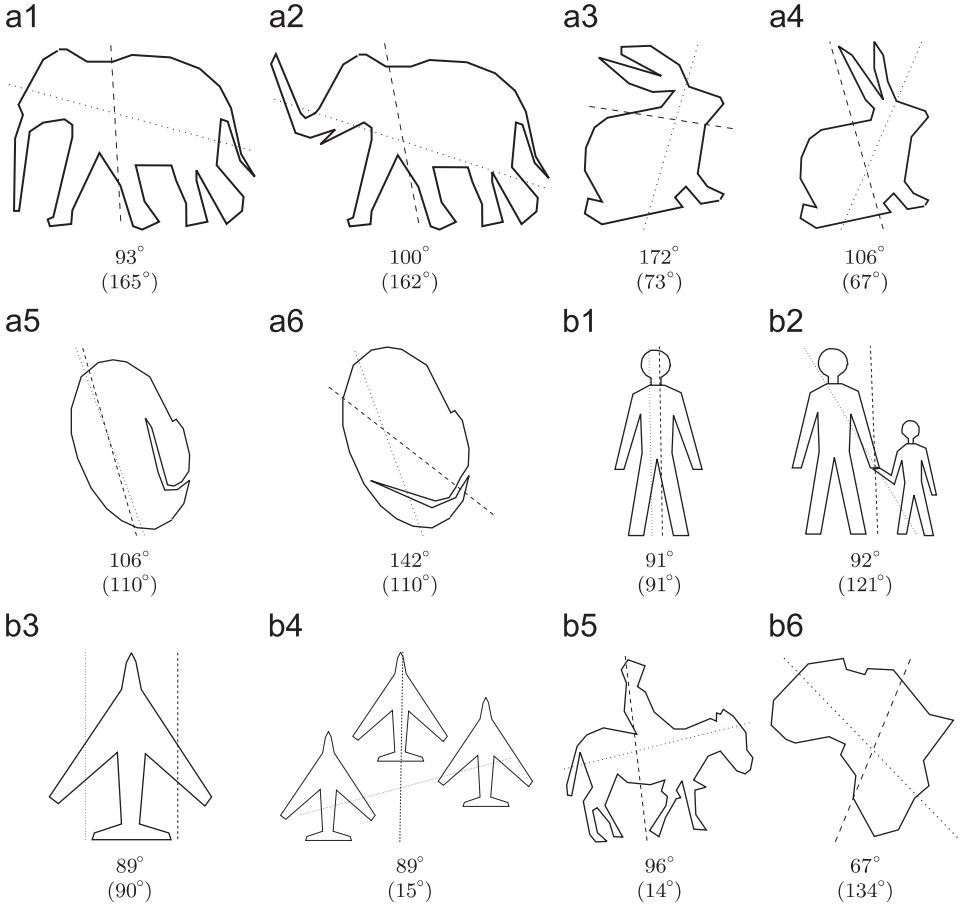

Fig. 3. Computed orientations $\mathcal{O}_{new}(P)$ are listed bellow shapes. Orientations $\mathcal{O}_{st}(P)$ computed by the standard method are in brackets. Dashed lines show $\mathcal{O}_{new}(P)$ orientations while dotted lines show $\mathcal{O}_{st}(P)$ orientations.

that consists of two silhouettes is oriented then the new method gives a very acceptable orientation of 92° while the standard method gives an unacceptable orientation of 121°. A similar situation arises with the next two shapes (b3) and (b4). While a single aircraft is properly oriented by both methods, a group of three aircraft is properly oriented by the new method while the standard method gives an unacceptable orientation. Because of importance, we point out this property by the following lemma.

Lemma 3.1. *If a compounded object consists of several polygonal shapes that have an identical orientation α_0 computed by the new method then the new method assigns the same orientation α_0 to the compounded object.*

Proof. Let Q be a compound object that consists of m polygonal shapes P_i, with $1 \leqslant i \leqslant m$. Then the function $F(\alpha, Q)$ can be expressed as $F(\alpha, Q) = \sum_{1 \leqslant i \leqslant m} F(\alpha, P_i)$. Since all the functions $F(\alpha, P_i)$ reach their maximum for $\alpha = \alpha_0$ we have $P(\alpha, Q) \leqslant \sum_{1 \leqslant i \leqslant m} F(\alpha_0, P_i)$. Finally, since for $\alpha = \alpha_0$ the function $P(\alpha, Q)$ reaches its upper bound given by the previous inequality, we establish the proof. □

The last two shapes in Fig. 3 (shapes (b5) and (b6)) present two cases where orientations computed by both methods differ, but it seems that there is no reason to prefer one of the methods.

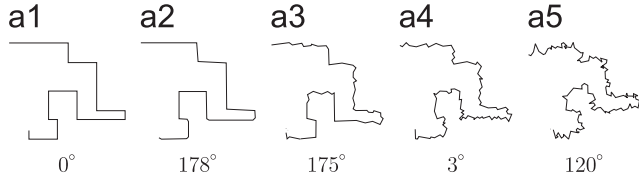

Fig. 4. Computed orientations $\mathcal{O}_{new}(P)$ are given to illustrate noise effects.

Since the new method is boundary based, it has to be very sensitive to the boundary defects (caused by a noise, for example). In Fig. 4 a polygonal line is presented in order to illustrate the possible noise effects on the computed orientation. Some low level noise effects can be corrected by a suitable choice of polygonal approximation (shape in the middle), but once again, big boundary defects (the last shape) must lead to an essential change in the computed orientation. Fig. 4 also illustrates that the method can be applied to the open polygonal lines.

The expectation that the orientation of a shape coincides with its axis of symmetry, should it have exactly one, is already discussed in relation with triangles $\triangle P_1P_2P_3$ and $\triangle P_1'P_2'P_3'$ from Fig. 1. As mentioned in the first instance, such a coincidence between the symmetry axis and shape orientation could seem

to be reasonable. But, considering a reflectively symmetric triangle with a very small height, a (triangle) orientation which is orthogonal to its axis of symmetry is more acceptable. Such an orientation is computed if the new method is applied (see Section 2).

The next theorem shows that the new method computes such an orientation if applied to an arbitrarily reflective symmetric shape. More precisely, the next lemma shows that the computed orientation of a reflective symmetric shape is either consistent or orthogonal to one of its symmetry axes (for some illustrations of the statement see Figs. 3 and 6).

Lemma 3.2. *Let P be a reflective symmetric polygonal shape, and let one of its symmetry axes have slope β. Then the total sum $F(\alpha, P)$ of squared projections of the edges of P onto a line reaches its maximum (minimum) either for $\alpha=\beta$ or $\alpha=\beta+\pi/2$, and consequently the computed orientation $\mathcal{O}_{new}(P)$ is either β or $\beta+\pi/2$.*

Proof. Without loss of generality we can assume that $\beta = 0$ i.e., the x-axis is one of the symmetry axes of P. The edges $e_1, e_2, \ldots, e_n$ of P can be divided into two disjoint groups that belong to two half planes determined by the x-axis. (If an edge intersects the x-axis it should be split onto two parts each one belonging to the opposing half planes.)

Let $e'_1, e'_2, \ldots, e'_m$ be edges lying above the x-axis and let α'_i be the corresponding angles between those edges and the x-axis.

Also, let $e''_1, e''_2, \ldots, e''_m$ be edges lying below the x-axis and let α''_i be the corresponding angles between those edges and the x-axis, such that

$$|e'_i| = |e''_i| \quad \text{and} \quad \alpha''_i = 180 - \alpha'_i \ \text{ for all } i = 1, 2, \ldots, m.$$

Then,

$$\begin{aligned}
F(\alpha, P) &= \sum_{e_i \ is \ an \ edge \ of \ P} |e_i|^2 \cos^2(\alpha_i - \alpha) \\
&= \sum_{i=1}^{m} |e'_i|^2 \cos^2(\alpha'_i - \alpha) + \sum_{i=1}^{m} |e''_i|^2 \cos^2(\alpha''_i - \alpha) \\
&= \sum_{i=1}^{m} |e'_i|^2 (\cos^2(\alpha'_i - \alpha) + \cos^2(180 - \alpha'_i - \alpha)) \\
&= 2 \cdot \sum_{i=1}^{m} |e'_i|^2 (\cos^2 \alpha'_i \cdot \cos^2 \alpha + \sin^2 \alpha'_i \cdot \sin^2 \alpha) \\
&= 2 \cdot \sum_{i=1}^{m} |e'_i|^2 \sin^2 \alpha'_i \\
&\quad + 2 \cdot \sum_{i=1}^{m} |e'_i|^2 (\cos^2 \alpha'_i - \sin^2 \alpha'_i) \cdot \cos^2 \alpha \\
&= \sum_{e_i \ is \ an \ edge \ of \ P} |e_i|^2 \sin^2 \alpha_i \\
&\quad + \sum_{e_i \ is \ an \ edge \ of \ P} |e_i|^2 (\cos^2 \alpha_i - \sin^2 \alpha_i) \cdot \cos^2 \alpha.
\end{aligned}$$

So, we distinguish three situations:

- $\sum_{e_i \ is \ an \ edge \ of \ P} |e_i|^2 \left(\cos^2\alpha_i - \sin^2\alpha_i\right) > 0$ then $F(\alpha, P)$ reaches its maximum for $\alpha = 0$ and the minimum for $\alpha = \pi/2$. The symmetry axis corresponds to the computed shape orientation.
- $\sum_{e_i \ is \ an \ edge \ of \ P} |e_i|^2 (\cos^2\alpha_i - \sin^2\alpha_i) < 0$ then $F(\alpha, P)$ reaches its minimum for $\alpha = 0$ and the maximum for $\alpha = \pi/2$. The symmetry axis is orthogonal to the computed shape orientation.
- $\sum_{e_i \ is \ an \ edge \ of \ P} |e_i|^2 (\cos^2\alpha_i - \sin^2\alpha_i) = 0$ then $F(\alpha, P)$ is a constant function. The minimum and maximum are the same and reached at any point. The method does not suggest what the orientation should be. □

4. Limitations of the method

Already presented examples illustrate that the new method gives reasonable orientations. On the other hand, it is already illustrated that there are some situations where the new method does not work. It has been already shown that the function $F(\alpha, P)$ is a constant function if P is a regular triangle or if P is a square. This implies that no direction could be pointed out as the shape orientation. Eqs. (6) are formal conditions that have to be satisfied if a polygonal shape cannot be oriented by the method presented here. There are many shapes, regular and irregular, that satisfy those criteria. A particular class of shapes whose orientation cannot be computed by the new method is the class of M-fold rotationally symmetric shapes ($M > 2$). The next lemma shows that for each polygonal shape having more than two axes of symmetry and more generally, each M-fold rotationally symmetric (with $M > 2$) shape P, the function $F(\alpha, P)$ is constant and consequently the shape orientation $\mathcal{O}_{new}(P)$ cannot be computed by the new method.

Lemma 4.1. *If a polygonal shape with boundary P is M-fold rotationally symmetric and if $M > 2$ then $F(\alpha, P)$ is a constant function.*

Proof. The proved equality (3) shows that there only four extreme points (two maxima and two minima) of the function $F(\alpha, P)$ on the interval $[0, 2\pi)$ or $F(\alpha, P)$ is constant. If P is M-fold rotationally symmetric with $M > 2$ then the function $F(\alpha, P)$ must have (at least) one minima and one maxima at each interval of the form

$$\left[(i-1) \cdot \frac{2\pi}{M}, i \cdot \frac{2\pi}{M}\right), \quad i = 1, \ldots, M$$

or it is a constant function. Because $M > 2$ is assumed there cannot be $2M$ strict extreme points, which implies that $F(\alpha, P)$ is constant. That establishes the proof. □

The result of the previous lemma is not a surprise. A similar situation occurs is if the standard method is applied—for details see [10,17]. Due to its simplicity, the function $F(\alpha, P)$ is not a

strong enough mathematical tool that can be used to define the orientation for many-fold rotationally symmetric shapes. It is worth mentioning that it is not expected for the orientation of M-fold rotationally symmetric shapes to be uniquely defined. The most natural result is to have M directions that concurrently define the shape orientation. The mutual angles between these directions should be $i \cdot 2\pi/M$ where $i = 1, \ldots, M$. Thus, if we would like to have a computable orientation for a wider shape class (that includes rotationally symmetric shapes) the method should be modified. The replacement of the exponent 2 in Eq. (2) with a bigger number seems to be a natural modification. We give the following definition.

Definition 4.1. Let P be a shape with a polygonal boundary. Then, the shape orientation $\mathcal{O}_{new,2N}(P)$ is defined by the angle α such that the total sum

$$F_{2N}(\alpha, P) = \sum_{e_i \text{ is an edge of } P} |\mathbf{pr}_{\vec{a}}(e_i)|^{2N} = \sum_{e_i \text{ is an edge of } P} |e_i|^{2N} \cos^{2N}(\alpha_i - \alpha) \quad (7)$$

of $2N$-powers of the lengths of the projections of the edges of P onto a line having the slope α is the maximal possible.

The "complexity" of $F_{2N}(\alpha, P)$ increases with an increase of N. In order to have $F_{2N}(\alpha, P) = constant$ the polygon P has to satisfy stronger criteria than in the case of $N = 2$. But due to the diversity of the shapes involved, as big exponent $2N$ is chosen it is always possible to find a polygon P such that $F_{2N}(\alpha, P)$ is constant, and consequently, the method cannot be used for the computation of the orientation of P. Particularly, M-fold rotationally symmetric shapes with $M > 2N$ are such shapes, as stated by the following theorem.

Theorem 4.1. *Let P be the boundary of an M-fold rotationally symmetric polygonal shape. Then $F_{2N}(\alpha, P)$ is constant if $2N < M$.*

Proof. Let P be an M-fold rotationally symmetric polygon. First, we will derive that there are not more than $4N$ values of α for which $\mathrm{d}F_{2N}(\alpha, P)/\mathrm{d}\alpha$ vanishes.

Indeed, starting from

$$\frac{\mathrm{d}F_{2N}(\alpha, P)}{\mathrm{d}\alpha} = \frac{\mathrm{d}(\sum_{e_i \text{ is an edge of } P} |e_i|^{2N}(\cos\alpha_i \cos\alpha + \sin\alpha_i \sin\alpha)^{2N})}{\mathrm{d}\alpha} = \sum_{e_i \text{ is an edge of } P} 2N \cdot |e_i|^{2N}(\cos\alpha_i \cos\alpha + \sin\alpha_i \sin\alpha)^{2N-1} \times (-\cos\alpha_i \sin\alpha + \sin\alpha_i \cos\alpha) \quad (8)$$

we distinguish two situations (denoted by (i) and (ii)) depending on the values of $\mathrm{d}F_{2N}(\alpha = 0, P)/\mathrm{d}\alpha$ and $\mathrm{d}F_{2N}(\alpha = \pi, P)/\mathrm{d}\alpha$:

(i) If $\alpha = 0$ and $\alpha = \pi$ (i.e. $\sin\alpha = 0$) are not solutions of $\mathrm{d}F_{2N}(\alpha, P)/\mathrm{d}\alpha = 0$, then we have from Eq. (8)

$$\frac{\mathrm{d}F_{2N}(\alpha, P)}{\mathrm{d}\alpha} = 0 \Leftrightarrow (\sin\alpha)^{2N} \times \sum_{e_i \text{ is an edge of } P} |e_i|^{2N}(\cos\alpha_i \cot\alpha + \sin\alpha_i)^{2N-1} \times (-\cos\alpha_i + \sin\alpha_i \cot\alpha) = 0.$$

Since the quantity

$$\sum_{e_i \text{ is an edge of } P} |e_i|^{2N}(\cos\alpha_i \cot\alpha + \sin\alpha_i)^{2N-1} \times (-\cos\alpha_i + \sin\alpha_i \cot\alpha) \quad (9)$$

is a $2N$-degree polynomial on $\cot\alpha$ it cannot have more than $2N$ real zeros

$$\cot\alpha_1 = z_1, \quad \cot\alpha_2 = z_2, \ldots, \quad \cot\alpha_k = z_k \quad (k \leqslant 2N).$$

Since $\cot\alpha = \cot(\alpha + \pi)$ we deduce that the equation

$$\frac{\mathrm{d}F_{2N}(\alpha, P)}{\mathrm{d}\alpha} = 0$$

has no more than $4N$ solutions, assuming that $F_{2N}(\alpha, P)$ is not a constant function.

(ii) If $\alpha = 0$ and $\alpha = \pi$ (i.e., $\sin\alpha = 0$) are solutions of $\mathrm{d}F_{2N}(\alpha, P)/\mathrm{d}\alpha = 0$, then (see Eq. (8))

$$\sum_{e_i \text{ is an edge of } P} |e_i|^{2N} \cdot \cos^{2N-1}\alpha_i \cdot \sin\alpha_i = 0. \quad (10)$$

But, in such a situation the quantity Eq. (9) is an $(2N-1)$-degree polynomial in $\cot\alpha$ since the coefficient of $(\cot\alpha)^{2N}$ vanishes (because of Eq. (10)). Consequently, the polynomial (9) cannot have more than $2N-1$ real zeros:

$$\cot\alpha_1 = z_1, \quad \cot\alpha_2 = z_2, \ldots, \quad \cot\alpha_k = z_k \quad (k \leqslant 2N-1),$$

i.e. there are no more than $2(2N-1) = 4N-2$ values of α for which the sum (9) (and consequently $\mathrm{d}F_{2N}(\alpha, P)/\mathrm{d}\alpha$) vanishes. So, again, including $\alpha = 0$ and $\alpha = \pi$, the total number of zeros of $\mathrm{d}F_{2N}(\alpha, P)/\mathrm{d}\alpha = 0$ is not bigger than $4N$.

Thus, in both cases ((i) and (ii)) the number of zeros of $\mathrm{d}F_{2N}(\alpha, P)/\mathrm{d}\alpha$ is upper bounded by $4N$.

On the other hand, if P is a fixed M-fold rotationally symmetric polygon, then $F_{2N}(\alpha, P)$ must have (because of the symmetry) at least M local minima and M local maxima (one minimum and one maximum at any interval of the form $[\alpha, \alpha + 2\pi/M)$, or it must be a constant function. That means that $\mathrm{d}F_{2N}(\alpha, P)/\mathrm{d}\alpha$ must have (at least) $2M$ zeros $\alpha_1, \alpha_2, \ldots, \alpha_{2M}$.

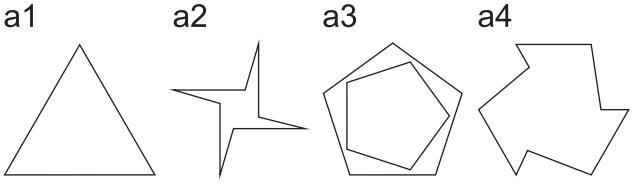

Fig. 5. Orientation of manifold rotational symmetric shapes.

Table 1
Orientations as computed by applying Definition 4.1 to the shapes from Fig. 5

	Fig. 5(a1)	Fig. 5(a2)	Fig. 5(a3)	Fig. 5(a4)
$\mathcal{O}_{new,2}(P)$	not computable	not computable	not computable	not computable
$\mathcal{O}_{new,4}(P)$	not computable	88°	not computable	not computable
$\mathcal{O}_{new,6}(P)$	0°	89°	not computable	172°
$\mathcal{O}_{new,8}(P)$	0°	90°	not computable	175°
$\mathcal{O}_{new,10}(P)$	0°	90°	0°	176°

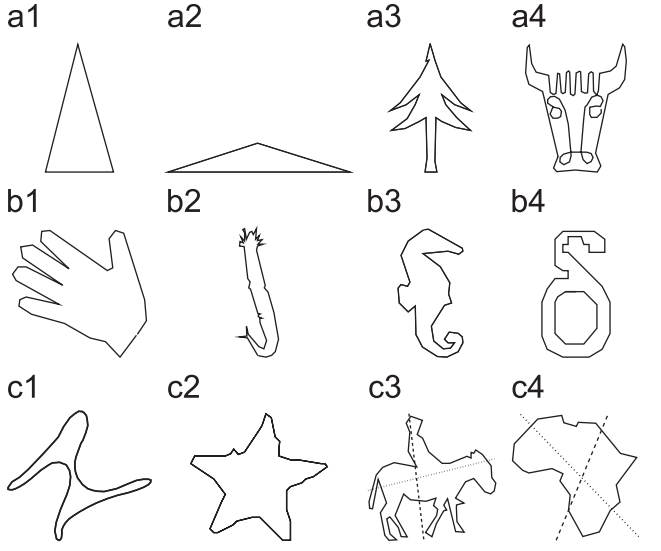

Fig. 6. Presented shapes are oriented by using $F_{2N}(\alpha, P)$ for different values of N. The obtained results are in Table 2.

Table 2
Orientations $\mathcal{O}_{new,2N}(P)$ are computed for the shapes from Fig. 6

	Fig. 6(a1)	Fig. 6(a2)	Fig. 6(a3)	Fig. 6(a4)
$\mathcal{O}_{new,2}(P)$	91°	0°	89°	91°
$\mathcal{O}_{new,4}(P)$	91°	0°	90°	93°
$\mathcal{O}_{new,6}(P)$	91°	0°	90°	95°
$\mathcal{O}_{new,8}(P)$	92°	0°	90°	98°
$\mathcal{O}_{new,10}(P)$	92°	0°	90°	99°
	Fig. 6(b1)	Fig. 6(b2)	Fig. 6(b3)	Fig. 6(b4)
$\mathcal{O}_{new,2}(P)$	140°	103°	127°	114°
$\mathcal{O}_{new,4}(P)$	137°	103°	144°	123°
$\mathcal{O}_{new,6}(P)$	134°	102°	149°	133°
$\mathcal{O}_{new,8}(P)$	134°	102°	150°	135°
$\mathcal{O}_{new,10}(P)$	138°	102°	151°	135°
	Fig. 6(c1)	Fig. 6(c2)	Fig. 6(c3)	Fig. 6(c4)
$\mathcal{O}_{new,2}(P)$	44°	10°	96°	67°
$\mathcal{O}_{new,4}(P)$	46°	178°	94°	126°
$\mathcal{O}_{new,6}(P)$	48°	178°	96°	128°
$\mathcal{O}_{new,8}(P)$	48°	179°	98°	128°
$\mathcal{O}_{new,10}(P)$	48°	179°	100°	129°

Since the presumption $2N < M$ does not allow $2M$ zeros of $\mathrm{d}F_{2N}(\alpha, P)/\mathrm{d}\alpha$ if $F_{2N}(\alpha, P)$ is not a constant function, we just derived a contradiction. So, $F_{2N}(\alpha, P)$ must be constant for all $2N$ less than M. □

Several many fold rotationally symmetric shapes are presented in Fig. 5, while their orientations computed based on $F_{2N}(\alpha, P)$ for $N = 1, 2, 3, 4$, and 5 are in Table 1. The results are in accordance with Theorem 4.1. A regular triangle (Fig. 5(a1)) cannot be oriented if $F_2(\alpha, P)$ and $F_4(\alpha, P)$ are used, while a use of $F_6(\alpha, P)$, $F_8(\alpha, P)$, and $F_{10}(\alpha, P)$ gives a 0° orientation—of course the orientations 120° and 240° are congruent to the orientation of 0° and $F_{2N}(0°, P) = F_{2N}(120°, P) = F_{2N}(240°, P)$ holds in the presented case. Just to mention that a modification of the standard method from [17] gives, a perhaps more acceptable, orientation of 60°. The shape in Fig. 5(a2) is 4-fold rotationally symmetric, and consequently cannot be oriented if $F_2(\alpha, P)$ is used. A use of $F_4(\alpha, P)$, $F_6(\alpha, P)$, $F_9(\alpha, P)$, and $F_{10}(\alpha, P)$ leads to acceptable results. The similar discussion is valid for the last two shapes in Fig. 5.

Irregular shapes in Fig. 6 are oriented by using $F_{2N}(\alpha, P)$ for different values of N. Shapes Fig. 6(a1)–(a4) are almost reflectively symmetric and their computed orientations are in accordance with Lemma 3.2 (if $F_2(\alpha, P)$ is used). The shape in Fig. 6(b2) seems to be "well orientable" (i.e. it has a distinct orientation) and that is the reason that there are no big variations in the computed orientation when $2N$ changes. The rest of the results are acceptable.

5. Orientation of shapes with arbitrary boundaries

In Section 2, a new method for the orientation of polygonal shapes was described. Many shapes are polygonal by nature: machine made products, crystals, house outlines on satellite images, etc. Also, many shapes can be efficiently approximated by polygonal shapes that have relatively few edges. In the initial version given by Definition 2.1, the method has some undesirable properties. One of them is that there are situations where the method does not work. Many-fold rotationally symmetric shapes are shapes that could not be oriented if the initial version is applied. A modification of the method is proposed (in the previous section) in order to overcome the apparent problems.

Another modification will be described in this section. It is motivated by the following natural question: *If a curve is replaced by a polygonal line whose vertices are sample points belonging to the curve, does the computed orientation* $\mathcal{O}_{new}(P)$ (*defined by Definition* 2.1) *converge when the maximum distance between consecutive points decrease to zero*? In other informal words, we consider whether the computed orientation of a curve (not necessarily a polygonal one) converges when the density of the curve sample points increases (see Fig. 7 for an illustration).

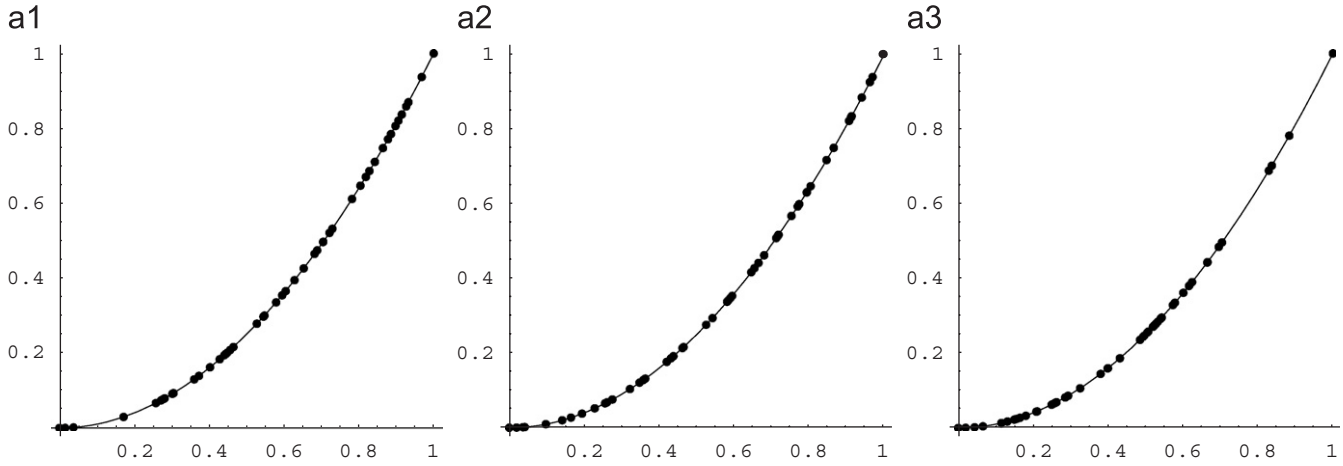

Fig. 7. Fifty randomly selected points (x_i, x_i^2) are displayed. The polygonal line $(0,0)=(x_1,x_1^2),(x_2,x_2^2),\ldots,(x_{49},x_{49}^2),(x_{50},x_{50}^2)=(1,1)$ is oriented by the new method. The following orientations are obtained: (a1) 40°; (a2) 48°; (a3) 56°.

We need some well-known mathematics to verify this. Taking into account trivial trigonometric identities

$$\sin(2\alpha)=\frac{2\tan\alpha}{1+\tan^2\alpha}\quad\text{and}\quad\cos(2\alpha)=\frac{1-\tan^2\alpha}{1+\tan^2\alpha}\tag{11}$$

and the fact that the first derivative $\dot{y}/\dot{x}=(\mathrm{d}y/\mathrm{d}t)/(\mathrm{d}x/\mathrm{d}t)$ of a curve given as $x=x(t),\ y=y(t)$ equals the tangent of the angle between the curve tangent and the x-axis, we obtain the following identities (12) and (13) that hold for piecewise smooth enough curves.

Lemma 5.1. *Let C be a piecewise smooth enough curve given in parametric form $x=x(t)$, $y=y(t)$ where $t\in[a,b]$. Let*

$$A_1=(x(t=a),y(t=a)),A_2,\ldots,A_{k-1},$$
$$A_k=(x(t=b),y(t=b))$$

be points from the curve C, and let α_i denotes the angle between the $\overrightarrow{A_iA_{i+1}}$ and the x-axis. Then

$$\lim_{\substack{k\to\infty\\ \max\{|A_iA_{i+1}|,1\leqslant i<k\}\to 0}}\sum_{i=1}^{k-1}|A_iA_{i+1}|\cdot\sin(2\alpha_i)$$
$$=\oint_C\frac{2\dot{x}\dot{y}}{\dot{x}^2+\dot{y}^2}\,\mathrm{d}s=\int_a^b\frac{2\dot{x}\dot{y}}{\sqrt{\dot{x}^2+\dot{y}^2}}\,\mathrm{d}t\tag{12}$$

and

$$\lim_{\substack{k\to\infty\\ \max\{|A_iA_{i+1}|,1\leqslant i<k\}\to 0}}\sum_{i=1}^{k-1}|A_iA_{i+1}|\cdot\cos(2\alpha_i)$$
$$=\oint_C\frac{\dot{x}^2-\dot{y}^2}{\dot{x}^2+\dot{y}^2}\,\mathrm{d}s=\int_a^b\frac{\dot{x}^2-\dot{y}^2}{\sqrt{\dot{x}^2+\dot{y}^2}}\,\mathrm{d}t.\tag{13}$$

Thus if the number of the points on the curve increase such that the maximum distance between consecutive points tends to zero, both quantities $\sum_{i=1}^{k-1}|A_iA_{i+1}|\cdot\sin(2\alpha_i)$ and $\sum_{i=1}^{k-1}|A_iA_{i+1}|\cdot\cos(2\alpha_i)$ converge, as given by (12) and (13).

Also, since

$$\left|\sum_{1\leqslant i<k}|A_iA_{i+1}|^2\cdot\sin(2\alpha_i)\right|\leqslant\max\{|A_iA_{i+1}|,1\leqslant i<k\}\times\sum_{1\leqslant i<k}|A_iA_{i+1}|\cdot\sin(2\alpha_i)$$

i.e.

$$\left|\sum_{1\leqslant i<k}|A_iA_{i+1}|^2\cdot\cos(2\alpha_i)\right|\leqslant\max\{|A_iA_{i+1}|,1\leqslant i<k\}\times\sum_{1\leqslant i<k}|A_iA_{i+1}|\cdot\cos(2\alpha_i)$$

and because of Eqs. (12), (13), and $\max\{|A_iA_{i+1}|,1\leqslant i<k\}\to 0$ we have

$$\lim_{\substack{k\to\infty\\ \max\{|A_iA_{i+1}|,1\leqslant i<k\}\to 0}}\sum_{i=1}^{k-1}|A_iA_{i+1}|^2\cdot\sin(2\alpha_i)=0,$$

$$\lim_{\substack{k\to\infty\\ \max\{|A_iA_{i+1}|,1\leqslant i<k\}\to 0}}\sum_{i=1}^{k-1}|A_iA_{i+1}|^2\cdot\cos(2\alpha_i)=0.$$

The quantities $\sum_{i=1}^{k-1}|A_iA_{i+1}|^2\cdot\sin(2\alpha_i)$ and $\sum_{i=1}^{k-1}|A_iA_{i+1}|^2\cdot\cos(2\alpha_i)$ actually appear in Eq. (3) and their ratio equals the tangent of the double angle that is the assigned orientation $\mathcal{O}_{new}(L)$ to the polygonal line L determined by the sample points. The convergence of such a ratio

$$\frac{\sum_{i=1}^{k-1}|A_iA_{i+1}|^2\cdot\sin(2\alpha_i)}{\sum_{i=1}^{k-1}|A_iA_{i+1}|^2\cdot\cos(2\alpha_i)}$$

is not guaranteed in a general case. That is illustrated by Fig. 7: Fifty points x_i are selected at random three times. The polygonal line having vertices $(0,0)=(x_1,x_1^2),\ (x_2,x_2^2),\ldots,(x_{49},x_{49}^2)$,

$(x_{50}, x_{50}^2)=(1, 1)$ is oriented by the new method. The following orientations are obtained:

- Fig. 7(a1). The computed orientation is 40°.
- Fig. 7(a2). The computed orientation is 48°.
- Fig. 7(a3). The computed orientation is 56°.

Note: The abscissas of the selected points are can be found in Ref. [22].

Starting from the trivial inequalities

$$\frac{\min\{|A_iA_{i+1}|, 1\leqslant i<k\}}{\max\{|A_iA_{i+1}|, 1\leqslant i<k\}}\cdot\frac{\sum_{1\leqslant i<k}|A_iA_{i+1}|\sin(2\alpha_i)}{\sum_{1\leqslant i<k}|A_iA_{i+1}|\cos(2\alpha_i)} \leqslant \frac{\sum_{1\leqslant i<k}|A_iA_{i+1}|^2\sin(2\alpha_i)}{\sum_{1\leqslant i<k}|A_iA_{i+1}|^2\cos(2\alpha_i)} \tag{14}$$

and

$$\frac{\sum_{1\leqslant i<k}|A_iA_{i+1}|^2\sin(2\alpha_i)}{\sum_{1\leqslant i<k}|A_iA_{i+1}|^2\cos(2\alpha_i)} \leqslant \frac{\max\{|A_iA_{i+1}|, 1\leqslant i<k\}}{\min\{|A_iA_{i+1}|, 1\leqslant i<k\}} \times\frac{\sum_{1\leqslant i<k}|A_iA_{i+1}|\sin(2\alpha_i)}{\sum_{1\leqslant i<k}|A_iA_{i+1}|\cos(2\alpha_i)} \tag{15}$$

we can see that the convergence of the computed orientations is guaranteed if

$$|A_iA_{i+1}|=|A_jA_{j+1}| \quad \text{for all } i, j \text{ from } \{1, 2, \ldots, k-1\} \tag{16}$$

holds. In such a case $\frac{\min\{|A_iA_{i+1}|,1\leqslant i<k\}}{\max\{|A_iA_{i+1}|,1\leqslant i<k\}}=\frac{\max\{|A_iA_{i+1}|,1\leqslant i<k\}}{\min\{|A_iA_{i+1}|,1\leqslant i<k\}}=1$ and consequently (by Eqs. (12)–(15)) the computed orientation converges to a fixed value α that satisfies

$$\tan(2\alpha)=\frac{\int_a^b\frac{2\dot{x}\dot{y}}{\sqrt{\dot{x}^2+\dot{y}^2}}\,dt}{\int_a^b\frac{\dot{x}^2-\dot{y}^2}{\sqrt{\dot{x}^2+\dot{y}^2}}\,dt}. \tag{17}$$

If Eq. (16) is not preserved we have the following estimate for computed orientations

$$\frac{1}{K}\cdot L\leqslant\tan(2\alpha)\leqslant K\cdot L, \tag{18}$$

where

$$K=\frac{\max\{|A_iA_{i+1}|, 1\leqslant i<k\}}{\min\{|A_iA_{i+1}|, 1\leqslant i<k\}}$$

and

$$L=\frac{\int_a^b\frac{2\dot{x}\dot{y}}{\sqrt{\dot{x}^2+\dot{y}^2}}\,dt}{\int_a^b\frac{\dot{x}^2-\dot{y}^2}{\sqrt{\dot{x}^2+\dot{y}^2}}\,dt}.$$

The problem is that it is very difficult (almost impossible in real applications) to preserve that Eq. (16) be satisfied. On the other hand, the described convergence would be a very nice property if working with shapes that are not polygonal by their nature or when working with shapes that do not have a simple (but reasonably good) polygonal representation.

In order to overcome such problems we define another shape orientation $\mathcal{O}_{mod}(P)$ which is actually a modification of $\mathcal{O}_{new}(P)$.

Definition 5.1. Let P be a shape with a polygonal boundary. The shape orientation $\mathcal{O}_{mod}(P)$ is defined by the angle α for which the total sum

$$G(\alpha, P)=\sum_{e\ is\ an\ edge\ of\ P}\frac{|\mathbf{pr}_{\vec{a}}(e)|^2}{|e|} =\sum_{e\ is\ an\ edge\ of\ P}|e|\cdot\cos^2(\alpha_i-\alpha) \tag{19}$$

reaches the maximum.

Table 3 shows orientations of shapes if they are oriented in accordance with Definition 5.1. As it can be seen from Table 3, orientations $\mathcal{O}_{new}(P)$ and $\mathcal{O}_{mod}(P)$ introduced by Definition 2.1 and Definition 5.1 perform similarly on the shapes presented on Figs. 3–6. A general conclusion that can be made is that the impact of the long edges is smaller in the case of a use of $\mathcal{O}_{mod}(P)$—which is natural since the edge lengths participate as a linear term in Definition 5.1 (see Eq. (19)) while they participate as a square term in Definition 2.1 (see also Eq. (4)). As an illustration, Fig. 8 displays the graphs of $F(\alpha, P)$ and $G(\alpha, P)$ where P is the boundary of the shape presented in Fig. 3(a6). The standard method gives the orientation 100° while the orientation $\mathcal{O}_{mod}$ is 142°, i.e. $F(\alpha, P)$ reaches the maximum for $\alpha=142°$. This change from 100° to 142° is caused by a deep, almost horizontal, intrusion. As expected, the impact of such an intrusion is smaller if $G(\alpha, P)$ is used (edge lengths participate as linear terms) and computed orientation $\mathcal{O}_{mod}$ is 130°, i.e. $G(\alpha, P)$ reaches the maximum for $\alpha=130°$. Just to mention that in the presented case (see Fig. 8),where the measure unit is actually the pixel size, $F(\alpha, P)$ varies approximatively between 3,745,000 and 8,000,000 while $G(\alpha, P)$ varies approximatively between 6690 and 9000. Since the edges of the presented shape are essentially bigger then 1 (i.e. bigger than the pixel size) such a much higher variation is expected in the case of $F(\alpha, P)$ where the edge length participate as squared quantities.

It is very important to notice that in all the cases presented in Fig. 7 the orientations computed by Definition 5.1 are consistent and all are equal to 46°—which illustrates the "convergence" property of this method. That can be understood as a big advantage with respect to the computations based on Definition 2.1 which give divergent orientations 40°, 48°, and 56°.

A few more examples are given in Fig. 9. Shapes (a1)–(a4) are by their nature presented by open lines. The last shape (a5) illustrates the application on the shape whose boundary is not completely extracted.

Based on the previous discussion we give a preference to the orientation $\mathcal{O}_{mod}(P)$ against the orientation $\mathcal{O}_{new}(P)$. The

Table 3
Shape orientations $\mathcal{O}_{mod}(P)$ computed by using Definition 5.1

Fig. 3(a1) 100°	Fig. 3(a2) 106°	Fig. 3(a3) 164°	Fig. 3(a4) 119°	Fig. 3(a5) 107°	Fig. 3(a6) 130°
Fig. 3(b1) 91°	Fig. 3(b2) 93°	Fig. 3(b) 89°	Fig. 3(b4) 89°	Fig. 3(b5) 100°	Fig. 3(b6) 40°
Fig. 4(a1) 0°	Fig. 4(a2) 175°	Fig. 4(a3) 171°	Fig. 4(a) 175°	Fig. 4(a5) 135°	
Fig. 5(a1) Not computable	Fig. 5(a2) Not computable	Fig. 5(a3) Not computable	Fig. 5(a4) Not computable		
Fig. 6(a1) 91°	Fig. 6(a2) 0°	Fig. 6(a3) 89°	Fig. 6(a4) 90°		
Fig. 6(b1) 142°	Fig. 6(b2) 102°	Fig. 6(b3) 124°	Fig. 6(b4) 112°		
Fig. 6(c1) 44°	Fig. 6(c2) 22°	Fig. 6(c3) 100°	Fig. 6(c4) 40°		
Fig. 7(a1) 46°	Fig. 7(a2) 46°	Fig. 7(a3) 46°			

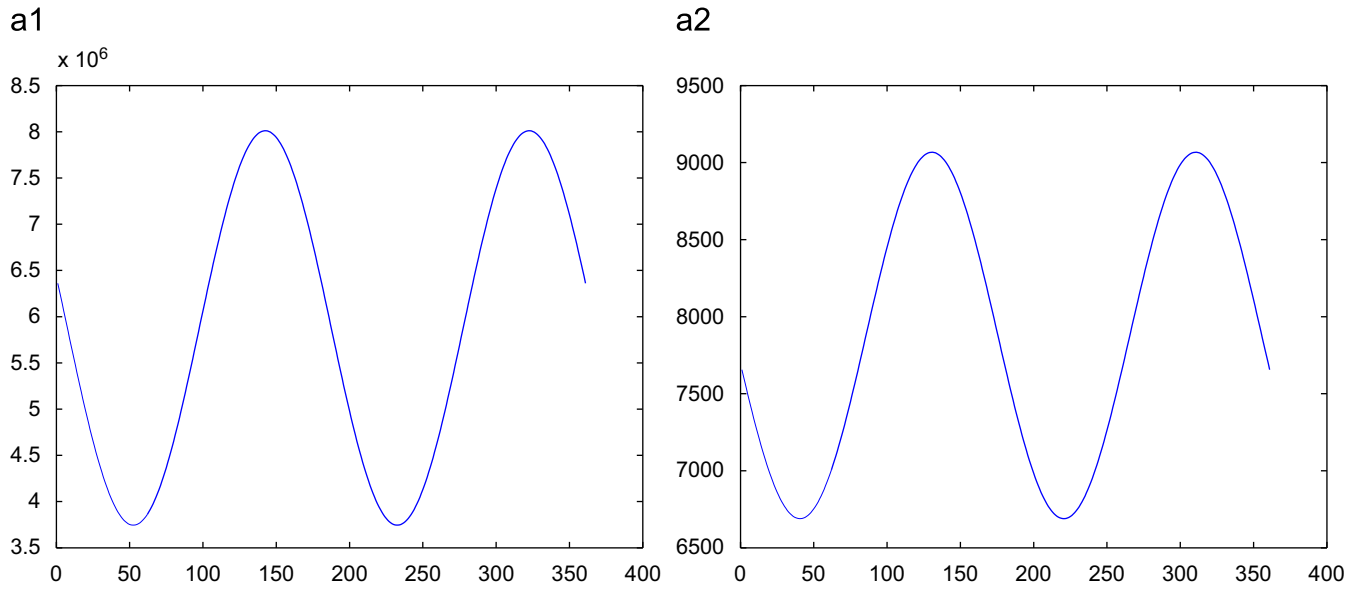

Fig. 8. The abscissas in both graphs measure the angle α in radians. The ordinate in (a1) measures $F(\alpha, P)$, while the ordinate in (a2) measures $G(\alpha, P)$—in both cases the measure unit equals the pixel size. P is the shape in Fig. 3(a6).

proved "convergence" property is the only reason for our choice.

Now, we give the following theorem that summarises the useful properties of $\mathcal{O}_{mod}(P)$. The proofs are omitted because of the analogy to the already proven statements.

Theorem 5.1. *Let C be a piecewise smooth enough curve given in parametric form $x = x(t)$, $y = y(t)$ where $t \in [a, b]$. Let $A_1{=}(x(t{=}a), y(t{=}a))$, $A_2, \ldots, A_{k-1}$, $A_k{=}(x(t{=}b), y(t{=}b))$ be points from the curve C while α_i denotes the angle between the edge $e_i = [A_i A_{i+1}]$ and the x-axis.*

If $A_1, A_2, \ldots, A_k$ are consecutive vertices of a polygonal line (not necessarily closed) P then:

(a) *The angle α for which the function $G(\alpha, P) = \sum_{e_i \text{ is an edge of } P} \frac{|\mathbf{pr}_{\vec{a}}(e_i)|^2}{|e_i|}$ reaches its maximum satisfies*

$$\tan(2 \cdot \alpha) = \frac{\sum_{e_i \text{ is an edge of } P} |e_i| \cdot \sin(2\alpha_i)}{\sum_{e_i \text{ is an edge of } P} |e_i| \cdot \cos(2\alpha_i)}; \tag{20}$$

(b) *If P is reflectively symmetric then the orientation $\mathcal{O}_{mod}(P)$ computed by the method defined by Definition 5.1 is*

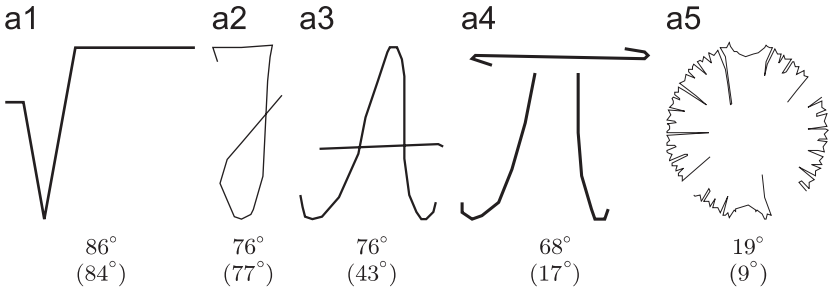

Fig. 9. Orientations $\mathcal{O}_{mod}(P)$ introduced by Definition 5.2 are below considered polygonal lines. Orientations $\mathcal{O}_{new}(P)$ are in brackets.

coincident with one of the symmetry axes of P or it is orthogonal to one of them;

(c) *If P is M-fold rotationally symmetric, with* $M > 2$, *then* $G(\alpha, P)$ *is a constant function and it cannot be used to compute the orientation of P*;

(d) *Let the number k of sample points* A_i *from the curve C increase such that* $\max\{|A_iA_{i+1}|, 1 \leqslant i < k\} \to 0$. *If* P_k *is the polygon line determined by the vertices* $A_1, A_2, \ldots, A_k$ *and if* $\overline{\alpha}_k$ *is the point where the function* $G(\alpha, P_k)$ *reaches the maximum then*

$$\lim_{\substack{k\to\infty \\ \max\{|A_iA_{i+1}|, 1\leqslant i<k\}\to 0}} \tan(2\overline{\alpha}_k) = \frac{\int_a^b \frac{2\dot{x}\dot{y}}{\sqrt{\dot{x}^2+\dot{y}^2}}\,\mathrm{d}t}{\int_a^b \frac{\dot{x}^2-\dot{y}^2}{\sqrt{\dot{x}^2+\dot{y}^2}}\,\mathrm{d}t}. \quad (21)$$

Because of item (d) of Theorem 5.1 it is natural to extend the applicability of the orientation $\mathcal{O}_{mod}(P)$ to the class of shapes with a smooth enough boundary (not necessarily polygonal) in the following way.

Definition 5.2. Let C be a shape with its boundary given in a parametric form: $x = x(t)$, $y = y(t)$ while $t \in [a, b]$. Then, the orientation $\mathcal{O}_{mod}(C)$ of C is given by

$$\tan(2\cdot\mathcal{O}_{mod}(C)) = \frac{\int_a^b \frac{2\dot{x}\dot{y}}{\sqrt{\dot{x}^2+\dot{y}^2}}\,\mathrm{d}t}{\int_a^b \frac{\dot{x}^2-\dot{y}^2}{\sqrt{\dot{x}^2+\dot{y}^2}}\,\mathrm{d}t}. \quad (22)$$

Remark 4. If C is a polygonal line (with edges e_i and the corresponding angles α_i $(1 \leqslant i \leqslant n)$), it can be also represented in the form $x = x(t)$, $y = y(t)$, $t \in [a, b]$. It is important to notice that the orientation of C can be computed by applying both formulas (20) and (22), i.e.,

$$\tan(2\cdot\mathcal{O}_{mod}(C)) = \frac{\sum_{i=1}^n |e_i|\cdot\sin(2\alpha_i)}{\sum_{i=1}^n |e_i|\cdot\cos(2\alpha_i)} = \frac{\int_a^b \frac{2\dot{x}\dot{y}}{\sqrt{\dot{x}^2+\dot{y}^2}}\,\mathrm{d}t}{\int_a^b \frac{\dot{x}^2-\dot{y}^2}{\sqrt{\dot{x}^2+\dot{y}^2}}\,\mathrm{d}t}.$$

holds. That is the reason why we use the same notation $\mathcal{O}_{mod}(P)$ in both Definitions 5.1 and 5.2.

We proceed with an example which illustrates the application of Definition 5.2 and the item (d) of Theorem 5.1 to a parabolic arc. Let us consider a parabola arc $C(v)$ given by $y = x^2$ and $x \in [0, v)$. In accordance with Definition 5.2, and by using the parametrisation $x = t$, $y = t^2$, $t \in [0, v)$, the orientation $\mathcal{O}_{mod}(C(v))$ of such an arc computed by (22) satisfies:

$$\tan(2\cdot\mathcal{O}_{mod}(C(v))) = \frac{\int_0^v \frac{2\dot{x}\dot{y}}{\sqrt{\dot{x}^2+\dot{y}^2}}\,\mathrm{d}t}{\int_0^v \frac{\dot{x}^2-\dot{y}^2}{\sqrt{\dot{x}^2+\dot{y}^2}}\,\mathrm{d}t} = \frac{\int_0^v \frac{4t}{\sqrt{1+4t^2}}\,\mathrm{d}t}{\int_0^v \frac{1-4t^2}{\sqrt{1+4t^2}}\,\mathrm{d}t}$$

$$= \frac{\sqrt{1+4v^2}-1}{\frac{3}{4}\ln(2v+\sqrt{1+4v^2}) - \frac{1}{2}v\sqrt{1+4v^2}}$$

(the graph of the function $\frac{\sqrt{1+4v^2}-1}{\frac{3}{4}\ln(2v+\sqrt{1+4v^2})-\frac{1}{2}v\sqrt{1+4v^2}}$ is in Fig. 10(a2)).

The limit values

$$\lim_{v\to 0} \frac{\sqrt{1+4v^2}-1}{\frac{3}{4}\ln(2v+\sqrt{1+4v^2}) - \frac{1}{2}v\sqrt{1+4v^2}}$$

$$= \lim_{v\to\infty} \frac{\sqrt{1+4v^2}-1}{\frac{3}{4}\ln(2v+\sqrt{1+4v^2}) - \frac{1}{2}v\sqrt{1+4v^2}} = 0$$

are in accordance with our expectation: For v very small (close to zero) the arc C has the orientation $\mathcal{O}_{mod}(C(v))$ very close to 0° but also that for a very large v the orientation $\mathcal{O}_{mod}(C(S))$ is close to 90°.

Further, the function $\frac{\sqrt{1+4v^2}-1}{\frac{3}{4}\ln(2v+\sqrt{1+4v^2})-\frac{1}{2}s\sqrt{1+4v^2}}$ has a discontinuity at $v_0 \approx 0.9799$ that corresponds to the value $v = v_0$ for which the arc $C(v_0)$ has the orientation $\mathcal{O}_{mod}(C(v_0)) = \pi/4$ (notice that then $\lim_{\varepsilon\to\pm 0}\tan(2\cdot\mathcal{O}_{mod}(C(v_0-\varepsilon))) = \pm\infty$). Since the standard definition of the function $\arctan(x)$ maps $(-\infty, \infty) \to (-\pi/2, \pi/2)$ the orientation $\mathcal{O}_{mod}(C(v))$ should

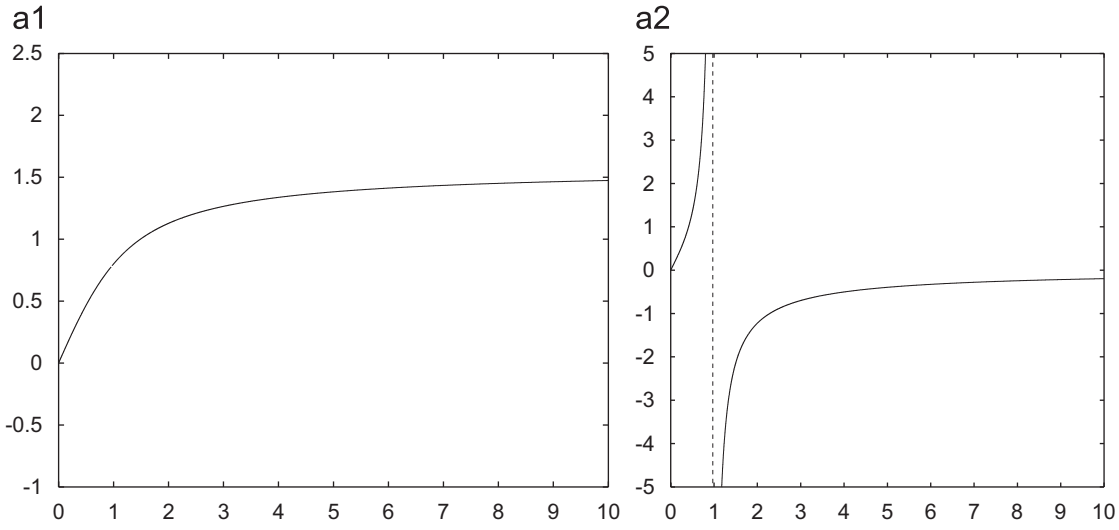

Fig. 10. (a1) The graph of the orientation $\mathcal{O}_{mod}(C(v))$ is displayed. (a2) The graph of the function $\frac{\sqrt{1+4v^2}-1}{\frac{3}{4}\ln(2v+\sqrt{1+4v^2})-\frac{1}{2}v\sqrt{1+4v^2}}$ is displayed.

be computed as

$$\mathcal{O}_{mod}(C(v)) = \begin{cases} \frac{1}{2}\arctan\left(\frac{\sqrt{1+4v^2}-1}{\frac{3}{4}\ln(2v+\sqrt{1+4v^2})-\frac{1}{2}v\sqrt{1+4v^2}}\right) \\ \text{if } v \in (0, v_0), \\ \frac{\pi}{2}+\frac{1}{2}\cdot\arctan\left(\frac{\sqrt{1+4v^2}-1}{\frac{3}{4}\ln(2v+\sqrt{1+4v^2})-\frac{1}{2}v\sqrt{1+4v^2}}\right) \\ \text{if } v\in(v_0, \infty). \end{cases}$$

The graph of the function $\mathcal{O}_{mod}(C(v))$ is in Fig. 10(a1).

6. Concluding remarks

In this paper we dealt with computing shape orientation based on the shape boundary. Initially we focused on shapes that have polygonal boundaries. That is not a strong restriction. In computer vision applications, we work with discrete data, which are very often approximated with canonical primitives in order to preserve more efficient image manipulation or a more efficient storage. The approximation of discrete shape boundaries with suitably chosen polygonal lines is a very common approach in practical applications, but circular arcs and splines of a given degree are also in use. As mentioned, we started with the orientation of polygonal shapes, but a later modification of the method enables us to evaluate the orientation of shapes with curved boundaries.

First we defined the orientation $\mathcal{O}_{new}(P)$ of a polygonal shape by the line that maximises the total sum of squared values of the length of projections of the edges of the shape boundary onto this line. That is a very natural definition that can also be applied directly to open polygonal lines, or to a set of such polygonal lines. This is an advantage when working with shapes whose boundaries are not extracted completely (because the shape pixels and background pixels are very similar, or because the considered object is partially overlaid, for example), or with shapes with characteristic scribble details that have to be taken into account when a shape is being oriented. Since the method is boundary based it is not expected to be particularly robust, but the sensitivity of the method could be an advantage in some particular applications (e.g. when working with high precision inspection tasks).

The computed orientation is demonstrated to be in accordance with human perception in some standard cases. For example, a computed orientation of a rectangle is coincident with its longer edge. The computed orientation of shapes with one symmetry axis is coincident with such an axis or it is orthogonal to it, etc.

The method is very simple to implement and moreover, it has been proven that such a defined shape orientation $\mathcal{O}_{new}(P)$ can be computed from a simple formula

$$\tan(2\cdot\mathcal{O}_{new}(P)) = \frac{\sum_{i=1}^{n}|e_i|^2\sin(2\alpha_i)}{\sum_{i=1}^{n}|e_i|^2\cos(2\alpha_i)}.$$

Comparing the above formula with Eq. (1) it can be said that the new method is not more complicated then the standard one.

Due to shape diversity it is expected that there is not a single method that works effectively in all situations. A simple characterisation of polygonal shapes whose orientation cannot be computed by the initial version of the method is given (see Eq. (6)). M-fold rotationally symmetric shapes ($M > 2$) are examples of shapes that cannot be oriented in such a way.

In order to extend a class of shapes that can be oriented, we have given a modification of the method. Instead of the squared length of the projections of the edges of the shape boundary we introduced a higher exponent. Precisely, we define the orientation $\mathcal{O}_{new,2N}(P)$ of a polygonal shape by a line that maximises the total sum of the lengths of edge projections taken with the power of $2N$. In such a way, a suitable choice of N can preserve a computable orientation of a higher class of shapes, but again, if the exponent $2N$ is fixed, there will always be shapes that cannot not be oriented. Such shapes are M-fold (with $M > 2N$) rotationally symmetric shapes, for example.

Finally, we come to the shape orientation $\mathcal{O}_{mod}(P)$ that satisfies an additional, very important, requirement. A modification of $\mathcal{O}_{new}(P)$ was needed because of the requirement that increasing the density of sample points from the shape boundary should lead to the convergence of the computed orientations. It has been shown that a slight modification of $\mathcal{O}_{new}(P)$ was enough to preserve such a requirement. Such a new defined orientation $\mathcal{O}_{mod}(P)$ has an additional benefit. It is the following simple equality:

$$\tan(2 \cdot \mathcal{O}_{mod}(C)) = \frac{\int_a^b \frac{2\dot{x}\dot{y}}{\sqrt{\dot{x}^2+\dot{y}^2}}\,\mathrm{d}t}{\int_a^b \frac{\dot{x}^2-\dot{y}^2}{\sqrt{\dot{x}^2+\dot{y}^2}}\,\mathrm{d}t}$$

that can be used for orientating shapes with curved boundaries C given in a parametric form $x = x(t)$, $y = y(t)$, $t \in [a, b]$. The above formula can be applied for open curve arcs as well. It is worth mentioning that in computer graphics and shape modelling area such curves (given in a parametric form) appear very often. But they could also appear in image processing tasks where pixel-based shape boundaries are sometimes needed to be approximated with parametric curved lines rather than by polygonal lines.

This paper also provides a set of experiments that should illustrate the proven statements and demonstrate how the method works in practice.

References

[1] B.K.P. Horn, Robot Vision, MIT Press, Cambridge, MA, 1986.

[2] R. Jain, R. Kasturi, B.G. Schunck, Machine Vision, McGraw-Hill, New York, 1995.

[3] R. Klette, A. Rosenfeld, Digital Geometry, Morgan Kaufmann, San Francisco, 2004.

[4] J. Cortadellas, J. Amat, F. de la Torre, Robust normalization of silhouettes for recognition application, Pattern Recognition Lett. 25 (2004) 591–601.

[5] V.H.S. Ha, J.M.F. Moura, Afine-permutation invariance of 2-D shape, IEEE Trans. Image Process. 14 (11) (2005) 1687–1700.

[6] J.-C. Lin, Universal principal axes: an easy-to-construct tool useful in defining shape orientations for almost every kind of shape, Pattern Recognition 26 (1993) 485–493.

[7] J.-C. Lin, The Family of Universal Axes, Pattern Recognition 29 (1996) 477–485.

[8] D. Shen, H.H.S. Ip, Generalized affine invariant normalization, IEEE Trans. Pattern Anal. Mach. Intell. 19 (5) (1997) 431–440.

[9] D. Shen, H.H.S. Ip, K.K.T. Cheung, E.K. Teoh, Symmetry detection by generalized complex (GC) moments: a close-form solution, IEEE Trans. Pattern Anal. Mach. Intell. 21 (5) (1999) 466–476.

[10] W.H. Tsai, S.L. Chou, Detection of generalized principal axes in rotationally symmetric shapes, Pattern Recognition 24 (1991) 95–104.

[11] S. Derrode, F. Ghorbel, Shape analysis and symmetry detection in gray-level objects using the analytical Fourier–Mellin representation, Signal Proc. 84 (2004) 25–39.

[12] W.-Y. Kim, Y.-S. Kim, Robust rotation angle estimator, IEEE Transactions on Pattern Analysis and Machine Intelligence 21 (8) (1999) 768–773.

[13] G. Marola, On the Detection of Axes of Symmetry of Symmetric and Almost Symmetric Planar Images, IEEE Trans. Pattern Anal. Mach. Intell. 11 (6) (1989) 104–108.

[14] V. Shiv Naga Prasad, B. Yegnanarayana, Finding axes of symmetry from potential fields, IEEE Trans. Image Processing 13 (12) (2004) 1556–1559.

[15] A. Taza, C.Y. Suen, Discrimination of planar shapes using shape matrices, IEEE Trans. System, Man and Cybernetics 19 (5) (1989) 1281–1289.

[16] S.E. Palmer, Vision Science: Photons to Phenomenology, MIT Press, 1999.

[17] J. Žunić, L. Kopanja, J.E. Fieldsend, Notes on shape orientation where the standard method does not work, Pattern Recognition 39 (5) (2006) 856–865.

[18] J. Žunić, P.L. Rosin, L. Kopanja, On the orientability of shapes, IEEE Transactions on Image Processing 15 (11) (2006) 3478–3487.

[19] H. Freeman, R. Shapira, Determining the minimum-area encasing rectangle for an arbitrary closed curve, Comm. of the ACM 18 (1975) 409–413.

[20] R.R. Martin, P.C. Stephenson, Putting objects into boxes, Computer Aided Design 20 (1988) 506–514.

[21] P.L. Rosin, Techniques for assessing polygonal approximations of curves, IEEE Trans. Pattern Anal. Mach. Intell. 19 (6) (1997) 659–666.

[22] M. Stojmenović, J. Žunić, New Measure for Shape Elongation, IbPRIA 2007, 3rd Iberian conference on pattern recognition and image analysis, Lecture Notes in Computer Science, vol. 4478, 2007, pp. 572–579.

About the Author—JOVISA ZUNIC received the M.Sc. and Ph.D. degrees in Mathematics and Computer Science from the University of Novi Sad (Serbia) in 1989 and 1991, respectively. He worked as a professor and researcher at the University of Novi Sad for more than a decade and is currently a senior lecturer in Department of Computer Science at Exeter University. He is also with the Mathematical Institute of the Serbian Academy of Sciences and Arts. He has been a visiting researcher at several universities—most recently, in the Tokyo Institute of Technology.
His research interest are in computer vision and image processing, digital geometry, shape representation and encoding of digital objects, discrete mathematics, combinatorial optimization, wireless networks, neural networks, and number theory.

About the Author—MILOS STOJMENOVIC received the Bachelor of Computer Science degree at the School of Information Technology and Engineering, University of Ottawa, in 2003. He obtained his Master's degree in computer science at Carleton University in Ottawa, Canada in 2005, and is now completing his Ph.D. in the same field at the University of Ottawa. He has a long list of awards for academic performance and medals from chess and math competitions. He published over a dozen articles in the fields of computer vision, image processing, and wireless networks. More details can be found at www.site.uottawa.ca/~mstoj075.